Distribution of Endothelial Cell Protein C/Activated Protein C Receptor (EPCR) During Mouse Embryo Development

James T.B. Crawley[1,2], Jian-Ming Gu[1,2], Gary Ferrell[1,2] and Charles T. Esmon[1,2,3]

Short title: EPCR in mouse development

[1]Cardiovascular Biology, Oklahoma Medical Research Foundation, OK 73104

[2]Howard Hughes Medical Institute, OK 73104

[3]Deparment of Pathology and Biochemistry & Molecular Biology, University of Oklahoma Health Sciences Center, OK 73190

Address correspondence to:

Dr Charles T. Esmon,
Howard Hughes Medical Institute,
Oklahoma Medical Research Foundation,
825 NE 13th Street,
Oklahoma City, OK 73104

E-mail: Charles-Esmon@omrf.ouhsc.edu
Tel: 405-271-7571
Fax: 405-271 3137

Selected abbreviations used:

APC - activated protein C, AP – alkaline phosphatase, EC – endothelial cell, EPCR – endothelial cell protein C/activated protein C receptor, FITC - fluorescein isothiocyanate, HRP – horseradish peroxidase, PBS – phosphate-buffered saline, TM – thrombomodulin, WT – wild-type,

Abstract

The endothelial cell protein C receptor (EPCR) augments the activation of protein C by the thrombomodulin· thrombin complex, leading to the feedback inhibition of thrombin generation. To examine whether EPCR might play a role during development, we performed an immunohistological analysis of EPCR distribution during mouse embryogenesis. EPCR was detected in the trophoblast giant cells at the feto-maternal boundary from embryonic day 7.5 (E7.5) and at later time points in the trophoblasts of the placenta, suggesting a role in the haemostatic regulation of the maternal blood that irrigates these surfaces. In the embryo proper, EPCR was weakly detected in aortic endothelial cells from E13.5. Thereafter, EPCR levels increased in certain large blood vessel endothelial cells and continued to rise until postnatal day 7, at which time the distribution mimicked that observed for adult mice. Taken together, these data suggest that the specificity of EPCR to large vessel endothelial cells is conferred *in utero*.

Key Words: EPCR, Development, Coagulation, Protein C, Thrombomodulin

Introduction

The protein C anticoagulant pathway represents one of the major regulatory mechanisms that modulate thrombin generation (1). Following the activation of coagulation, thrombin is generated rapidly at the site of vascular perturbation, culminating in the formation of a fibrin clot. At sites of intact endothelium, thrombin can bind to the integral membrane protein, thrombomodulin (TM) (2). In binding TM, the ability of thrombin to proteolytically activate protein C is greatly enhanced whereas its specificity for fibrinogen is lost (3). Activated protein C (APC), in conjunction with its co-factor, protein S, phospholipids and calcium ions, degrades clotting factors VIIIa and Va in the tenase and prothrombinase complexes respectively. In this way, further generation of thrombin can be attenuated.

A further component of the protein C anticoagulant pathway is the endothelial cell protein C receptor (EPCR) (4). EPCR is a type I transmembrane glycoprotein that binds protein C/APC with high affinity (K_d ~30nM), mediated largely via interactions with the Gla-domain of the latter (5, 6). In humans and baboons, EPCR is expressed predominantly by endothelial cells (EC) of larger blood vessels (7). With exception of the sinusoidal capillaries in the liver, the microvasculature appears to produce little or no EPCR. In addition, a 43kDa soluble form of EPCR (sEPCR), lacking the transmembrane region, is found in plasma under normal conditions (~2.5nM) (8). This arises as a result of the shedding of cellular EPCR by a metalloproteinase. Shedding is up-regulated *in vitro* in response to agonists such as thrombin or interleukin-1β (9). EC-surface EPCR augments the activation of protein C by TM·thrombin by reducing the K_m for this reaction (10, 11). This function appears physiologically important as the K_m for the activation of protein C by TM·thrombin in the absence of EPCR (~1μM) is significantly higher than the normal plasma concentration of protein C (~65nM) (12, 13). Indeed, in baboons, the specific antibody-mediated blocking of protein C binding to EPCR reduces protein C activation in response to thrombin infusion more than 10-fold (14).

We have recently performed targeted ablation of the *EPCR* gene in mice (15). Similar to the fate of TM knockout mice (16), the disruption of the *EPCR* gene in mice induces early post-implantation lethality in homozygous EPCR-deficient embryos (15). EPCR null embryos uniformly succumb to this lethal phenotype, which is associated with an increase in fibrin deposition, around embryonic day 9.5 (E9.5). This indicates that EPCR function in embryonic-derived cells is essential for normal mouse embryo development. To further characterize the role of EPCR in development and to assist the interpretation of the phenotypes exhibited by EPCR-deficient and certain EPCR transgenic mice, we undertook a comprehensive analysis of the distribution of this receptor in wild-type (WT) mouse embryos, neonates and adult mice.

Methods

Mouse Tissues

Timed WT mouse matings were set up and the developmental progress of embryos estimated by the gestational age, with day 0.5 post coitum defined as the morning of the vaginal plug. Pregnant female mice were sacrificed by carbon dioxide asphyxiation from E7.5 to E20.5 and placental/embryonic tissues removed. The generation and characterization of the homozygous EPCR-deficient embryos, used as a negative control for the immunostaining will be documented in a separate publication. Adult (>60 days) and new-born (1-day & 7-day) mice were sacrificed and organs/organ fragments removed. All tissues were washed briefly with phosphate-buffered saline (PBS), fixed in 4% paraformaldehyde/PBS at 4˚C for 2 hours and cryo-protected in 0.5M sucrose/PBS. Finally, specimens were mounted in OCT compound (R A Lamb), snap-frozen in liquid nitrogen-cooled isopentane and stored at –80˚C.

Northern Blot Analysis

For mouse embryonic tissues, a mouse embryo MTN™ mRNA blot containing mRNA extracted from E7.0, E11.0, E15.0 and E17.0 embryos was purchased (Clontech). For maternal tissues, RNA was extracted from decidual tissues between E7.5 and E11.5 and mRNA prepared using the Oligotex mRNA mini kit (Qiagen). 1μg of maternal uterine mRNA from each time point was separated on a 1% agarose gel containing formaldehyde and transferred onto a Hybond-N^+ membrane (AmershamPharmacia). Membranes were hybridized separately using full length, ^{32}P-labelled murine EPCR, TM and actin cDNA probes as previously described (4).

Antibodies

Two rat monoclonal (1560 and 1559 - both IgG_{2b}), and a goat polyclonal antibody (17), all reactive with murine EPCR were prepared by immunization using a soluble form of murine EPCR and subsequently affinity purified using immobilized murine sEPCR and standard techniques as previously

described (10). For the detection of TM, a polyclonal rabbit anti-murine TM (a gift from Dr E Conway) was used. A rat anti-murine CD31 (IgG_{2b}) (BD Pharmingen) was used as an EC-marker.

Non-immune rat IgG_{2b} (BD Pharmingen), rabbit IgG (Vector) and preimmune goat serum were used as negative controls. Primary antibodies were detected using either rabbit anti-rat IgG (mouse-absorbed), rabbit anti-goat or goat IgG anti-rabbit IgG antibodies conjugated to either biotin, fluorescein isothiocyanate (FITC) or Texas Red (Vector). Biotinylated antibodies were detected using streptavidin coupled to either horseradish peroxidase (HRP), alkaline phosphatase (AP) or Texas Red (Vector) depending on the staining technique employed.

Immunohistochemistry

Immunostaining was performed upon serially cut sections (8μm). Briefly, cryosections were fixed with 4% paraformaldehyde/PBS for 3 minutes and washed with PBS. As appropriate, endogenous peroxidase or AP activity was quenched using 1% hydrogen peroxide/PBS or 0.2M hydrogen chloride, respectively. Sections were rinsed and incubated with 0.1M glycine/PBS before incubation with blocking buffer (2% bovine serum albumin/2% normal serum/PBS) containing avidin/biotin blocking reagents (Vector) according to manufacturer's instructions. Sections were rinsed with PBS and incubated with primary antibody diluted in blocking buffer at 4˚C overnight. Thereafter, sections were washed with PBS and incubated with secondary antibody for 1 hour. Sections were washed as before, then for immunofluorescent detection, sections were mounted using Vectorshield containing the blue nuclear counter-stain, Dapi. For chromogenic detection, sections were incubated with the appropriate tertiary conjugate, washed with PBS and incubated with either DAB (HRP substrate - brown) or Vector Red (AP substrate) as appropriate and counter-stained with haematoxylin. Vector Red was viewed as a red reaction product by bright-field microscopy or as an intense red color by fluorescence microscopy. Images in the results section are frequently depicted with both fluorescent and bright-field micrographs of the same field to allow clear visualization of both specific staining and tissue morphology.

Results

EPCR in Early Post-Implantation Development (E7.5-E9.5)

At E7.5, comparatively high amounts of EPCR and TM were detected in the ECs throughout the maternal decidua (Fig.1 A&E). Decidual cells in the compact layer stained variably for EPCR, whereas those in the spongy layer exhibited little or no staining (Fig.1 A&C). The embryonic trophectoderm-derived trophoblast giant cells at the interface between maternal and embryonic tissues, were positive for both EPCR and TM. However, at E7.5 only TM was detected in the parietal and visceral yolk sac. Neither EPCR nor TM was evident in the embryo proper at this developmental stage.

Between E8.5 and E10.5, the staining for EPCR in the maternal decidual cells of the compact layer (Fig.1 F) became stronger and more homogeneous than at E7.5. The decidual cells of the spongy layer were negative for both EPCR (Fig.1 E) and TM (not shown), but the CD31-positive ECs lining the venous sinusoids in this region stained strongly for both receptors.

At E9.5, the trophoblast giant cells of the trophectoderm were clearly distinguishable (by their size and large nuclei) from the adjacent maternal decidual cells. EPCR was detected in all primary and secondary giant cells that surround the embryonic space and underlie the developing placenta. Frequently, the staining for both EPCR and TM appeared to preferentially decorate the surface of these cells, consistent with the distribution of these receptors on plasma membranes.

Some specimens (E9.5-E10.5) exhibited weak staining for EPCR in the single cell layered parietal endoderm lining Reichert's membrane, although EPCR was not generally detected in these cells until E11.5 (Fig.2 C&D). At no developmental time was EPCR detected in the yolk sac.

EPCR in Placental Development (E10.5-E20.5)

At E10.5, the spongiotrophoblasts, located at the shoulders and towards the maternal aspect of the placenta, were generally negative for both EPCR and TM (Fig.2 A&B). Maternal ECs (identified by the presence of biconcave, anuclear red blood cells in the lumen of these vessels) that lined microvessels in this region expressed both EPCR and TM. The embryonic ECs in the labyrinthine zone

underlying the chorionic plate (identified by the presence of nucleated red blood cells within these vessels) were positive for TM but not EPCR.

From E10.5, the maternal decidua diminished markedly in thickness. In the spongy decidual layer, EPCR was confined to ECs. As at earlier time points, decidual cells of the compact layer were strongly positive for EPCR and remained so throughout pregnancy (Fig.2 C).

At E11.5, EPCR in the developing chorioallantoic placenta was detected in the trophoblast cells at the maternal-embryonic boundary (Fig.2 C&E). The spongiotrophblasts were negative or stained weakly for EPCR at this time, but still interspersed with a few maternally-derived, EPCR-positive ECs. With time, maternal ECs were displaced by the trophoblasts in the placenta and thereafter were restricted to the venous sinusoids within the decidual layers

Between E12.5-E13.5, the staining for EPCR in spongiotrophoblasts became stronger. During this period, the syncytiotrophoblasts form the villous structures that comprise the murine placental labyrinth. These cells line the lumen of the placental sinuses into which the maternal blood flows from the uterine artery. They therefore correspond to the interface between the maternal and embryonic circulations. By double immunofluorescence (Fig.2 F-H), the allantoic ECs, identified by CD31-staining (green), were negative for EPCR. These cells could be clearly distinguished from the trophoblast cells of the placental labyrinth, which were positive for EPCR (red). As the labyrinth become more elaborate, the intensity of staining for EPCR (red) in the trophoblasts surrounding the placental ECs became stronger (compare Fig.2 F-H, E13.5-E15.5).

EPCR in the Developing Mouse Cardiovascular System

During the early stages of mouse organogenesis (E8-E11), the myocardial plate containing numerous ECs, detected by staining for CD31, could be clearly identified (Fig.3 A). EPCR, detected on serial section, was not detected in embryonic ECs in this or any other location at this time (Fig.3 B). TM however, was found in these and other embryonic ECs (also other cell types - neuronal cells, keratinocytes, lung epithelia, bone marrow as previously reported (16) - not shown),

At E13.5, by immunofluorescence, very weak staining for EPCR was first observed in the cells lining the lumen of the aorta (not shown) but not in any other embryonic vessels. At later time-points (E16.5-E18.5), staining for EPCR in the ECs of the aorta and the vena cava became more evident, though still weak (Fig.3 C&D). By E20.5, just prior to birth, the EC-staining for EPCR remained confined to the ECs of the aorta, vena cava and some smaller arteries/veins in the chest of the embryos (Fig.3 E). In 1-day neonatal mouse pups the endocardium of the heart remained negative for EPCR, whereas the adjacent aortic ECs were clearly positive (Fig.3 F). The presence of EPCR in both of these locations in 1-week old (not shown) and adult mice (Fig.3 G&H) suggested an up-regulation of *EPCR* expression during the first week after birth.

EPCR in the Vasculature of Other Organs

During embryogenesis, EPCR was not detected in the vasculature of the lungs or liver (not shown). Interestingly, EPCR was also absent from these locations in neonatal mice (Fig.4 A&C), where by double immunofluorescence for EPCR and CD31, only positive staining for CD31 (green) was observed. In 1-week old and adult mice, the larger vessels of the lung, but not the alveolar capillaries, stained strongly for EPCR (Fig.4 B). A similar increase in EPCR staining was observed in the liver of 1-week and adult mice (Fig.4 D). Here, the endothelium of the hepatic artery, central veins and sinusoidal capillaries all stained positively for EPCR.

In the neonatal mouse kidney, the larger vessels stained moderately for EPCR, whereas the ECs of the glomeruli were consistently negative (Fig.4 E), similar to the staining observed in adult mice (Fig.4 F). In the brain, EPCR was detected at comparable levels in veins, but not capillaries, of both neonatal and adult mice (Fig.4 G&H) of neonates. As a general observation, EPCR was more readily detectable in adult mice than mice in new-born pups.

Northern Blot Analysis

Northern blot data from mRNA extracted from E7.0-17.0 embryonic tissues (Fig 5) indicated both EPCR and TM were strongly expressed in mouse embryonic tissue during early post-implantation development. The E7.0 RNA sample was extracted from the embryo proper and trophectoderm, E11.0 to E17.0 RNA samples were extracted from the embryo proper alone (i.e. excluding the placenta). EPCR and TM mRNA detected at E7.0 most likely originate from the giant cells of the trophectoderm, which stained strongly for both antigens. Thereafter, EPCR transcripts were detected at very low levels between E11.0 and E17.0, consistent with its low level expression in selected large blood vessels. TM expression appeared to increase between E11.0 and E17.0 consistent with previous reports (16).

The presence of EPCR and TM transcripts in the maternal tissues is in accordance with the immunostaining data. At early time points, EPCR and TM were primarily located in the ECs of the decidual venous sinusoids. TM remained confined to this location in the mother throughout pregnancy, accounting for the minimal change in TM expression levels between E7.5-E11.5. EPCR however, was also strongly detected in the decidual cells of the compact layer, particularly after E7.5.

Discussion

In this study, we describe the distribution of EPCR during mouse development. In mouse maternal uterine tissues, EPCR was strongly detected in the endothelium of the large venous sinusoids in the spongy decidual layer. The cells of the compact decidual layer also stained strongly for EPCR. Interestingly, staining for TM in these decidual cells was either very weak or absent, possibly suggesting an alternative role for EPCR, independent of protein C activation. The distribution of EPCR in the maternal cells did not appear to change markedly during pregnancy.

During early post-implantation development (E7.5-E9.5), the primary and secondary trophoblast giant cells of the mural and polar trophectoderm were the only embryonic cells in which EPCR was detected. Trophoblast giant cells arise from the epithelial trophectoderm cells of the blastocyst. Following implantation these cells transform into invasive cells that displace and phagocytose the maternal decidua and make vascular connections with the maternal blood supply (18). The network of blood sinuses that form at the periphery of the embryo are lined on the side that faces Reichert's membrane by a single layer of trophoblast giant cells. These cells are highly flattened and fenestrated, facilitating diffusion of nutrients and oxygen to the embryonic region, allowing growth of the embryo prior to formation of the definitive chorioallantoic placenta. The presence of both EPCR and TM on the surface of giant cells suggest that, in this location, EPCR functions in augmenting protein C activation and the subsequent modulation of maternal thrombin generation. Between E6.5 and E7.5, maternal blood drains from the maternal decidua and surrounds the embryonic implantation site. The trophoblasts, representing the outermost layer of embryonic tissue, become exposed to the maternal circulation and its clotting factors, suggesting a requirement for haemostatic control in this location.

The disruption of the *TM* gene in mice leads to early embryonic lethality (16). The uniform death of $TM^{-/-}$ embryos around E8.5 has been linked to the absence of this receptor from the trophoblasts (19, 20). In addition, tissue factor, the initiator of coagulation, is expressed at the feto-maternal border (21), which most likely contributes to a hypercoagulable environment at this interface. Furthermore, it has

been reported that the elimination of tissue factor expression "rescues" TM null embryos from their early developmental death (16). Although, uncontrolled thrombin generation in the microenvironment of the trophoblast cells as a consequence of *TM* gene deletion has not been demonstrated directly, it seems likely that tight haemostatic regulation at the feto-maternal border is required (19). Given the importance for TM in trophoblasts, our findings in this report are consistent with EPCR, which augments protein C activation by TM•thrombin, fulfilling an anticoagulant function on the surface of these cells. In this study, we show the absence of EPCR from the trophoblast giant cells of EPCR null embryos as a control for the immunostaining results. The generation and characterization of the lethal phenotype exhibited by these embryos and the consequence of the ablation of EPCR expression from the trophoblasts will be reported in a later publication.

After E10.5, EPCR was detected in the parietal endoderm. This structure, which is not present in humans, represents a single cell layer lining Reichert's membrane that separates the trophoblast giant cells and the yolk sac. By E11.5 the chorioallantoic placenta is well formed. At this time, EPCR was confined to the trophoblasts at the outermost edge of the placenta in close proximity to the decidual cells. A few maternally-derived, EPCR-positive ECs could be identified at the shoulders of the spongy zone, but with time these were displaced. From E12.5, the embryonic vasculature of the placenta became more extensive; networks of embryonic blood vessels could be seen to pervade from the top of the chorionic plate. These vessels, which were devoid of detectable EPCR, are interspersed by villous structures formed by the syncytiotrophoblasts of the labyrinth. These trophoblasts separate the maternal blood from the embryonic ECs and function by modulating the exchange of oxygen, nutrients and waste products. The trophoblasts in this location were found to stain strongly for EPCR from E12.5.

EPCR in the embryo proper was not detected until around E13.5, when very weak staining in the aortic endothelium was first observed. At this time, the embryonic heart and vascular system are functional, which might suggest that the actions of EPCR are unlikely critical for early vascular morphogenesis.

However, we cannot exclude the possibility that trace amounts of EPCR (below the detection limits of this study) may have a functional role prior to this time.

By E16.5, EPCR staining in the aorta was stronger and the ECs of the vena cava were also positive. Thereafter, ECs of certain large arteries and veins, particularly in the vicinity or the rib primordia also exhibited EPCR expression. The specificity of EPCR expression for larger vessels has been attributed to the requirement for the augmentation of protein C activation in locations where the blood volume to endothelial surface ratio is high (i.e. in larger vessels). Furthermore unlike TM, which is expressed by a variety of non-endothelial cell types during development (16), EPCR expression in the embryo proper appeared to maintain its endothelial specificity. It will be of interest to ascertain how this specificity is manifest and by which promoter elements in the *EPCR* gene (22).

EPCR in new-born mice was absent from the hepatic and pulmonary vasculature and also the endocardium. Only during the first week after birth did EPCR expression elaborate such that it was distributed in the endothelium of all the major arteries and veins in a pattern analogous to that previously described for humans and baboons (7).

In conclusion, we propose that the distribution of EPCR during mouse development suggests an important role for EPCR in placental function, very possibly in the control of maternal thrombin generation. These findings will prove useful not only for interpreting the lethal phenotype exhibited by EPCR-deficient but also understanding the characteristics of EPCR transgenic mouse models generated in our laboratory.

Acknowledgements

This research was supported by a Specialized Centers of Research grant awarded by the National Institute of Health (#P50 HL54502). Charles T. Esmon is an investigator for the Howard Hughes Medical Institute.

References

1. Esmon CT. Regulation of blood coagulation. Biochim Biophys Acta. 2000;1477:349-60.

2. Esmon CT, Owen WG. Identification of an endothelial cell cofactor for thrombin-catalyzed activation of protein C. Proc Natl Acad Sci U S A. 1981;78:2249-52.

3. Esmon CT, Esmon NL, Harris KW. Complex formation between thrombin and thrombomodulin inhibits both thrombin-catalyzed fibrin formation and factor V activation. J Biol Chem. 1982;257:7944-7.

4. Fukudome K, Esmon CT. Identification, cloning, and regulation of a novel endothelial cell protein C/activated protein C receptor. J Biol Chem. 1994;269:26486-91.

5. Nishioka J, Ido M, Hayashi T, Suzuki K. The Gla26 residue of protein C is required for the binding of protein C to thrombomodulin and endothelial cell protein C receptor, but not to protein S and factor Va. Thromb Haemost. 1996;75:275-82.

6. Regan LM, Mollica JS, Rezaie AR, Esmon CT. The interaction between the endothelial cell protein C receptor and protein C is dictated by the gamma-carboxyglutamic acid domain of protein C. J Biol Chem. 1997;272:26279-84.

7. Laszik Z, Mitro A, Taylor FB Jr, Ferrell G, Esmon CT. Human protein C receptor is present primarily on endothelium of large blood vessels: implications for the control of the protein C pathway. Circulation. 1997;96:3633-40.

8. Kurosawa S, Stearns-Kurosawa DJ, Hidari N, Esmon CT. Identification of functional endothelial protein C receptor in human plasma. J Clin Invest. 1997;100:411-8.

9. Xu J, Qu D, Esmon NL, Esmon CT. Metalloproteolytic release of endothelial cell protein C receptor. J Biol Chem. 2000;275:6038-44.

10. Stearns-Kurosawa DJ, Kurosawa S, Mollica JS, Ferrell GL, Esmon CT. The endothelial cell protein C receptor augments protein C activation by the thrombin-thrombomodulin complex. Proc Natl Acad Sci U S A. 1996;93:10212-6.

11. Fukudome K, Ye X, Tsuneyoshi N, Tokunaga O, Sugawara K, Mizokami H, Kimoto M. Activation mechanism of anticoagulant protein C in large blood vessels involving the endothelial cell protein C receptor. J Exp Med. 1998;187:1029-35.

12. Owen WG, Esmon CT. Functional properties of an endothelial cell cofactor for thrombin-catalyzed activation of protein C. J Biol Chem. 1981;256:5532-5.

13. Galvin JB, Kurosawa S, Moore K, Esmon CT, Esmon NL. Reconstitution of rabbit thrombomodulin into phospholipid vesicles. J Biol Chem. 1987;262:2199-205.

14. Taylor FB Jr, Stearns-Kurosawa DJ, Kurosawa S, Ferrell G, Chang AC, Laszik Z, Kosanke S, Peer G, Esmon CT. The endothelial cell protein C receptor aids in host defense against Escherichia coli sepsis. Blood. 2000;95:1680-6.

15. Gu J-M, Ferrell G, Esmon CT: Targeted Disruption of the Endothelial Cell Protein C Receptor (EPCR) Causes Early Embryonic Lethality in Mice. Blood 2000;96:814a(Abstract)

16. Healy AM, Rayburn HB, Rosenberg RD, Weiler H. Absence of the blood-clotting regulator thrombomodulin causes embryonic lethality in mice before development of a functional cardiovascular system. Proc Natl Acad Sci U S A. 1995;92:850-4.

17. Gu JM, Katsuura Y, Ferrell GL, Grammas P, Esmon CT. Endotoxin and thrombin elevate rodent endothelial cell protein C receptor mRNA levels and increase receptor shedding in vivo. Blood. 2000;95:1687-93.

18. Bevilacqua EM, Abrahamsohn PA. Ultrastructure of trophoblast giant cell transformation during the invasive stage of implantation of the mouse embryo. J Morphol. 1988;198:341-51.

19. Isermann B, Hendrickson SB, Hutley K, Wing M, Weiler H. Tissue-restricted expression of thrombomodulin in the placenta rescues thrombomodulin-deficient mice from early lethality and reveals a secondary developmental block. Development. 2001;128:827-38.

20. Isermann B, Hendrickson SB, Zogg M, Wing M, Cummiskey M, Kisanuki YY, Yanagisawa M, Weiler H. Endothelium-specific loss of murine thrombomodulin disrupts the protein C anticoagulant

pathway and causes juvenile-onset thrombosis. J Clin Invest. 2001;108:537-46.

21. Luther T, Flossel C, Mackman N, Bierhaus A, Kasper M, Albrecht S, Sage EH, Iruela-Arispe L, Grossmann H, Strohlein A, Zhang Y, Nawroth PP, Carmeliet P, Loskutoff DJ, Muller M. Tissue factor expression during human and mouse development. Am J Pathol. 1996;149:101-13.

22. Gu JM, Fukudome K, Esmon CT. Characterization and regulation of the 5'-flanking region of the murine endothelial protein C receptor gene. J Biol Chem. 2000;275:12481-8.

Figure Legends

Figure 1 EPCR and TM in mouse uterine and embryonic tissues during early post-implantation development. Frozen tissue sections were stained for EPCR (A, C & F) or TM (E) using the Vector Red AP chromogenic immunodetection technique (see methods). As the positive red signal observed in bright field images (that show tissue morphology) is more evident by fluorescence microscopy, images are shown in pairs corresponding to both captured images of the same field of view. Tissue specimens depicted are WT mouse maternal/embryonic tissues harvested at E7.5 (A, B, D & E), E9.5 (F). The specimen depicted in panel C is a homozygous EPCR-deficient E7.5 embryo used solely as a control for the specificity of the anti-EPCR antibodies used.

At E7.5, EPCR (A) was detected in maternal ECs (*mec*) lining the venous sinusoids in the uterus. The decidual cells (*dc*) of the spongy layer were negative for EPCR. EPCR was also detected in the trophobasts of the trophectoderm surrounding the embryo, but not in any other embryonic cells at this time (dotted line represents the boundary between embryonic and maternally derived tissues). Staining of homozygous EPCR-deficient embryos (C) confirmed the specificity of the antibodies used against EPCR - note the absence of staining from the embryonic giant cells of the trophectoderm. The distribution of EPCR in the uterine ECs of the heterozygous EPCR-deficient mother mimics that observed for WT mice. Staining specificity was further confirmed by the negative staining of sections incubated with non-immune isotype control antibodies (B & D). TM (E) displayed a similar distribution as EPCR at this stage in development, with the exception of the yolk sac, which stained positive for TM but not EPCR (A). At E9.5, the embryo proper remained negative for EPCR (F), whereas strong staining of the decidual cells of the compact layer could be seen. EPCR in the spongy layer was confined to the sinusoidal ECs in this region. Scale bars=200μm. Key:- *dc*-decidual cells, *E*-embryo, *mec*-maternal endothelial cells, *gc*-trophoblast giant cells, *ys*-yolk sac.

Figure 2 Immunodetection of EPCR (A, C-H) and TM (B) during midgestation. Frozen tissue sections were stained for EPCR, TM and CD31 (EC-marker) by immunoperoxidase (A & B), immunophosphatase (C-E) and double immunofluorescence (F-H) techniques (see Methods). Tissue specimens depicted are maternal/embryonic tissues harvested at E10.5 (A&B), E11.5 (C-E), E13.5 (F), E14.5 (G) and E15.5 (H). At E10.5, the giant cells (*gc*), identified by their large nuclei, were strongly positive for both EPCR (A) and TM (B). Note the positive staining for EPCR, but not TM, in the maternal decidual cells of the compact layer. In the placenta, the spongiotrophoblasts at the shoulders of the allantoic placenta were negative for EPCR at this time, these embryonic cells were interspersed with a few EPCR- and TM-positive maternal ECs. In the labyrinthine zone underlying the chorionic plate, TM but not EPCR was detected in the embryonic ECs. Similarly, the ECs of the yolk sac vasculature and the parietal endoderm cells lining Reichert's membrane stained positive for TM (B) but not EPCR (A). At E11.5 (C-E), EPCR distribution in the maternal tissues remained as described at E9.5. In the chorioallantoic placenta, EPCR staining was confined to the maternal ECs at the edge of the spongy zone. Staining for EPCR in the cells of the parietal endoderm - a single cell layer lining the Reichert's membrane - became evident in all specimens around E11.5 (C&D).

At E13.5, by double immunofluorescence, EPCR (red) was detected in the trophoblasts (*t*) of the placental labyrinth but absent from the CD31-positve (green) embryonic ECs. The intensity of staining for EPCR increased in the trophoblasts with time (E14.5 - G, E15.5 - H) as the embryonic placental vasculature became more elaborate. EPCR remained undetectable in placental or umbilical ECs. Key:- *dc*-decidual cells, *E*-embryo, *eec*-embryonic ECs, *eUA-embryonic umbilical artery*, *mec*-maternal ECs, *gc*-trophoblast giant cells, *lz*-labyrinthine zone, *pe*-parietal endoderm, *sz*-spongy zone, *t*-trophoblasts, *ys*-yolk sac.

Figure 3 EPCR in the developing murine cardiovascular system. Frozen tissue sections were stained for EPCR and/or CD31 (EC-marker) by immunophosphatase (A & B) and immunofluorescence (C-H) techniques (see Methods). Tissue specimens depicted are maternal/embryonic tissues harvested at E10.5 (A-C), E16.5 (C & D), E20.5 (E) and tissue fragment harvested from 1-day postnatal (F) and adult (>60 days) mice (G & H). At E10.5, the developing heart could be easily identified morphologically, but also by the intense staining for CD31 that labeled the network of ECs (*eec*) in this region (A). In this image, staining for CD31 in the yolk sac ECs, giant cells and also the maternal decidual cells can be seen. On an adjacent serial section, staining for EPCR (B) was absent from the embryonic ECs of the yolk sac and developing heart. EPCR was first detected in aortic ECs at E13.5 (not shown). By immunofluorescence, staining for EPCR (red - arrowheads) in the cells lining the lumen of the aorta (C) and vena cava (D) became more evident at E16.5. By double immunofluorescence for EPCR (red - arrowheads) and CD31 (green) at E20.5, just prior to birth, EPCR was also detected in the endothelium of some vessels in close proximity to the ribs (E). In 1-day postnatal mouse pups, EPCR was clearly seen in aortic ECs, but not in the vasculature or endocardium of the heart (F). In adult mice, EPCR was readily detectable in large vessel ECs (vena cava & aorta -G) and the endocardium (H).

Figure 4 Double immunofluorescent detection of EPCR and CD31 (EC-marker) in selected organs of 1-day mouse neonates (A, C, E & G - left panel) and adult mice (B, D, F & H). Frozen tissue sections were stained using a mixture of anti-CD31 and anti-EPCR antibodies (see Methods). CD31 is represented in green and EPCR in red. In 1-day neonatal mice, EPCR was not detected in the pulmonary vasculature (A), whereas it was readily detectable the ECs of intraacinar and intraalveolar arteries and veins (B-arrowheads) stained in parallel. EPCR was not however found in the alveolar capillaries of adult mouse lungs. In the liver, EPCR was similarly absent from the hepatic vasculature of 1-day pups (C) but present in both the large vessels and sinusoidal capillaries (*sc*) of the adult mouse liver (D). In the kidney of both neonates (E) and adult mice (F), moderate EPCR staining was observed in the largest arteries and veins (arrowheads), but not the smaller vessels or glomerular capillaries (boxed areas). The distribution of EPCR in the larger vessels (arrowheads) (but not capillaries) in the brain was similar for both neonates (G) and adult mice (H)

Key:- *sc*-sinusoidal capillaries

Figure 5 Northern blot analysis of EPCR, TM and actin transcripts in mRNA extracted from mouse embryos (E7.0-E17.0) and the surrounding maternal decidua (E7.5-E11.5). The embryonic mRNA blot was purchased, mRNA from maternal tissue was prepared by the authors. Blots were hybridized separately with full-length ^{32}P-labelled EPCR and TM cDNA probes. Equal mRNA loading was established using a cDNA probe for actin.

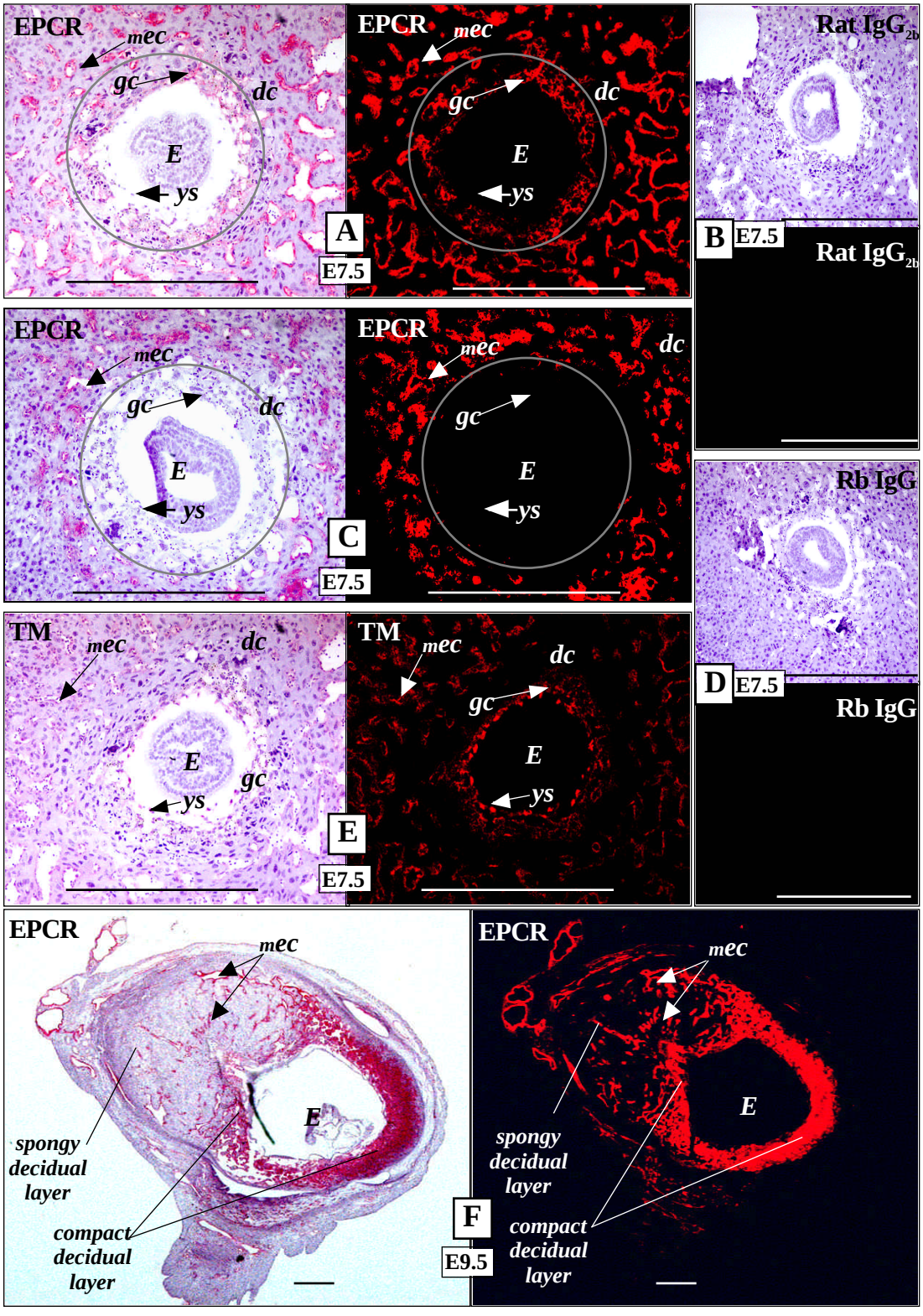
EPCR
mec
gc
dc
E
ys
A
E7.5
EPCR
mec
gc
dc
E
ys
Rat IgG2b
B
E7.5
Rat IgG2b
EPCR
mec
gc
dc
E
ys
C
E7.5
EPCR
mec
dc
gc
E
ys
Rb IgG
D
E7.5
Rb IgG
TM
mec
dc
E
gc
ys
E
E7.5
TM
mec
dc
gc
E
ys
EPCR
mec
E
spongy decidual layer
compact decidual layer
EPCR
mec
E
spongy decidual layer
compact decidual layer
F
E9.5

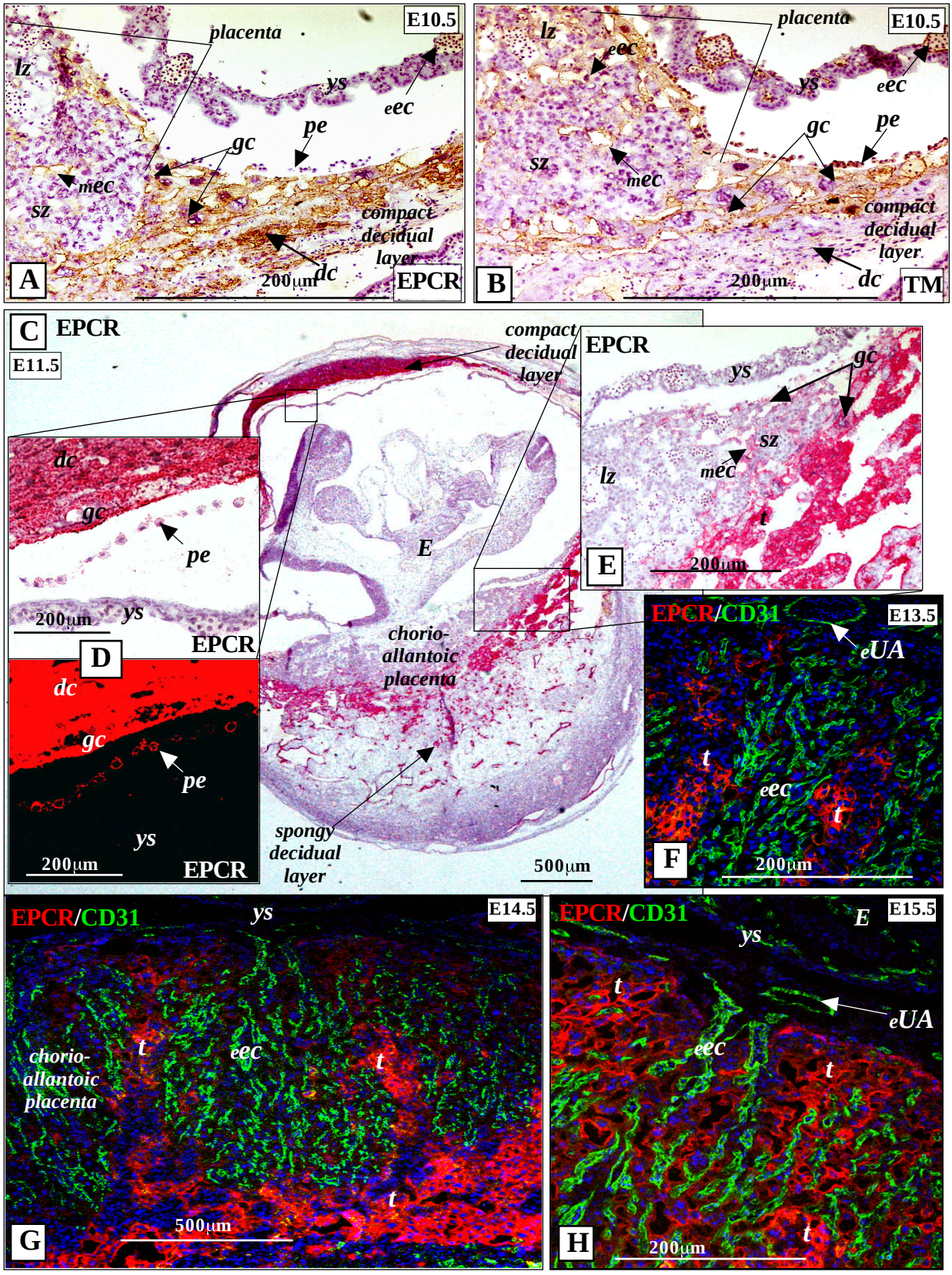
A
E10.5
placenta
lz
ys
eec
pe
gc
mec
sz
compact decidual layer
dc
200μm
EPCR
B
E10.5
placenta
lz
eec
ys
eec
gc
pe
sz
mec
compact decidual layer
dc
200μm
TM
C
EPCR
E11.5
compact decidual layer
dc
gc
pe
200μm
ys
EPCR
D
dc
gc
pe
ys
200μm
EPCR
E
chorio-allantoic placenta
spongy decidual layer
500μm
EPCR
ys
gc
sz
lz
mec
t
E
200μm
EPCR/CD31
E13.5
eUA
t
eec
t
F
200μm
EPCR/CD31
ys
E14.5
chorio-allantoic placenta
t
eec
t
t
G
500μm
EPCR/CD31
E
E15.5
ys
t
eUA
eec
t
t
H
200μm

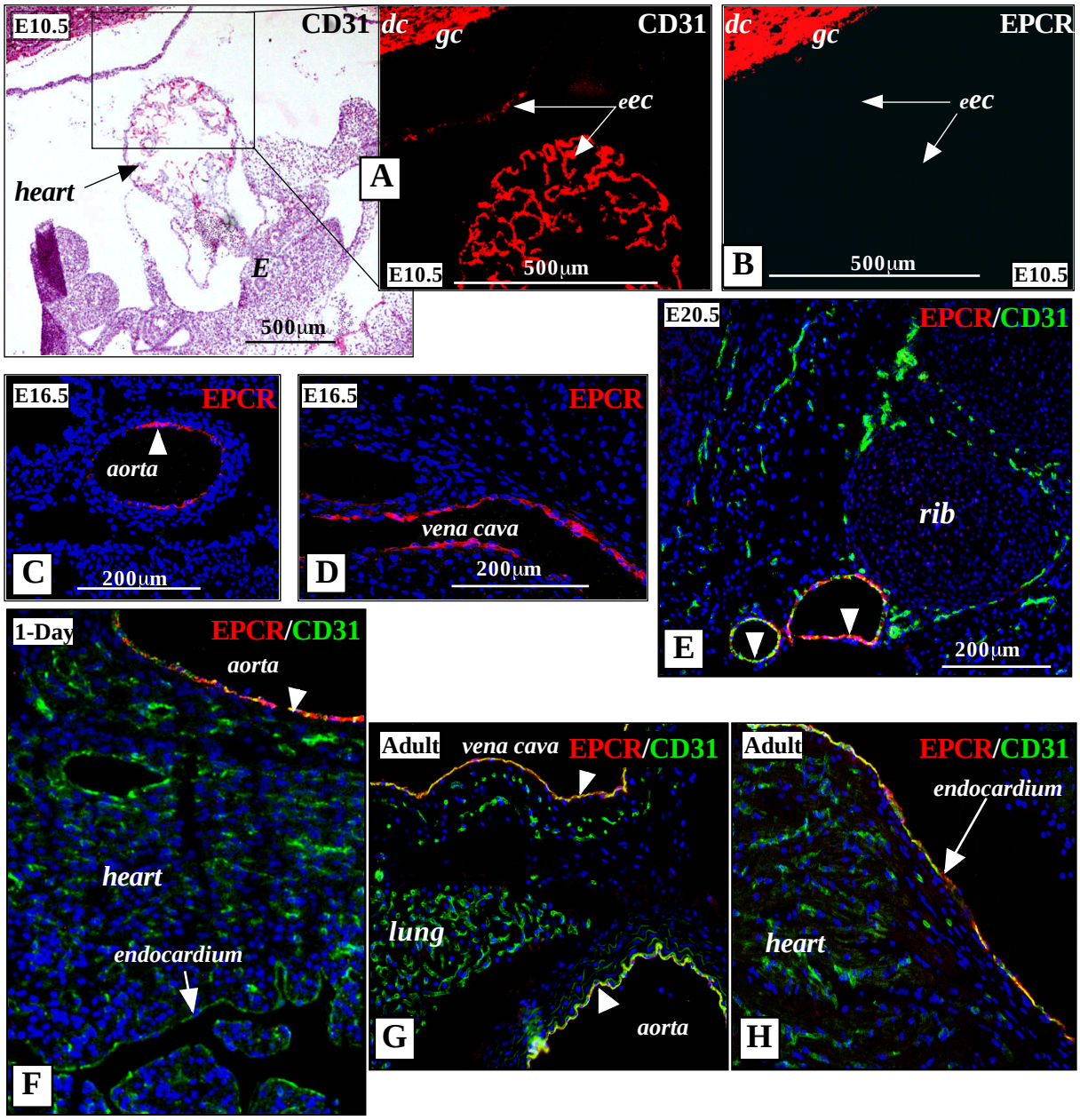
E10.5
CD31
heart
E
500μm
dc
gc
CD31
eec
A
E10.5
500μm
dc
gc
EPCR
eec
B
500μm
E10.5
E20.5
EPCR/CD31
rib
E
200μm
E16.5
EPCR
aorta
C
200μm
E16.5
EPCR
vena cava
D
200μm
1-Day
EPCR/CD31
aorta
heart
endocardium
F
Adult
vena cava
EPCR/CD31
lung
aorta
G
Adult
EPCR/CD31
endocardium
heart
H

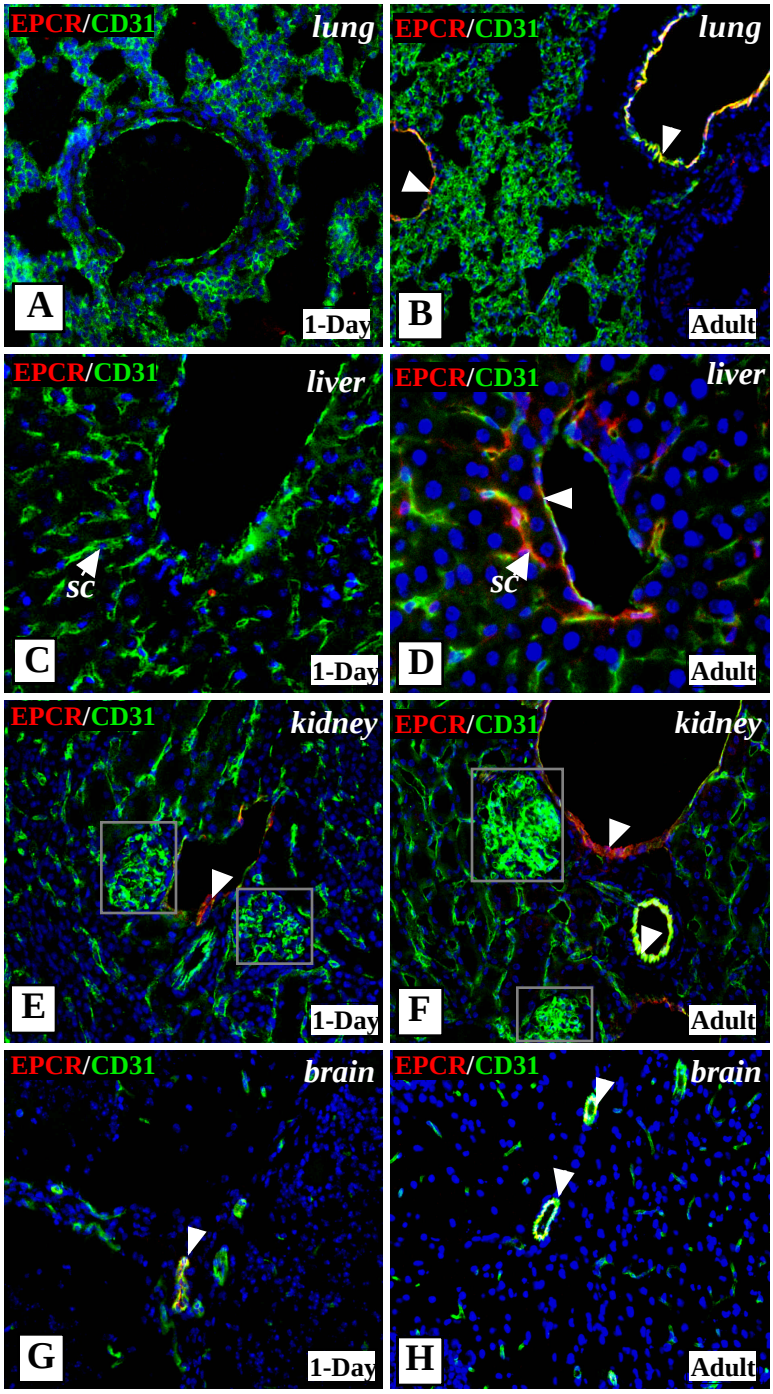
EPCR/CD31
lung
A
1-Day
EPCR/CD31
lung
B
Adult
EPCR/CD31
liver
sc
C
1-Day
EPCR/CD31
liver
sc
D
Adult
EPCR/CD31
kidney
E
1-Day
EPCR/CD31
kidney
F
Adult
EPCR/CD31
brain
G
1-Day
EPCR/CD31
brain
H
Adult

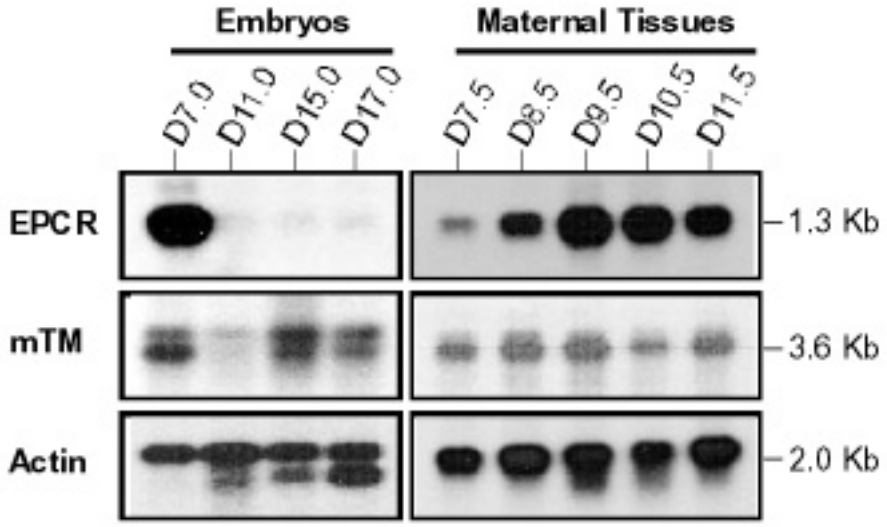
Embryos
Maternal Tissues
D7.0
D11.0
D15.0
D17.0
D7.5
D8.5
D9.5
D10.5
D11.5
EPCR
mTM
Actin
1.3 Kb
3.6 Kb
2.0 Kb